AFML-TR-76-87

FG

12

AN ANALYTICAL METHOD FOR EVALUATING IMPACT DAMAGE ENERGY OF LAMINATED COMPOSITES

PURDUE UNIVERSITY
SCHOOL OF AERONAUTICS AND ASTRONAUTICS
WEST LAFAYETTE, INDIANA 47907

S/C 291850

JUNE 1976

FINAL REPORT FOR PERIOD MAY 1974 - MAY 1975

AIR FORCE MATERIALS LABORATORY
AIR FORCE WRIGHT AERONAUTICAL LABORATORIES
AIR FORCE SYSTEMS COMMAND
WRIGHT-PATTERSON AIR FORCE BASE, OHIO 45433

LB

NOTICE

When Government drawings, specifications, or other data are used for any purpose other than in connection with a definitely related Government procurement operation, the United States Government thereby incurs no responsibility nor any obligation whatsoever; and the fact that the government may have formulated, furnished, or in any way supplied the said drawings, specifications, or other data, is not to be regarded by implication or otherwise as in any manner licensing the holder or any other person or corporation, or conveying any rights or permission to manufacture, use, or sell any patented invention that may in any way be related thereto.

This report has been reviewed by the Information Office (IO) and is releasable to the National Technical Information Service (NTIS). At NTIS, it will be available to the general public, including foreign nations.

This technical report has been reviewed and is approved for publication.

J. M. Whitney
J. M. Whitney
Project Monitor

FOR THE DIRECTOR

S. W. Tsai
S. W. Tsai, Chief
Mechanics & Surface Interactions Branch
Nonmetallic Materials Division

Copies of this report should not be returned unless return is required by security considerations, contractual obligations, or notice on a specific document.

AIR FORCE - 17 SEPTEMBER 76 - 175

UNCLASSIFIED

SECURITY CLASSIFICATION OF THIS PAGE (When Data Entered)

REPORT DOCUMENTATION PAGE	READ INSTRUCTIONS BEFORE COMPLETING FORM
1. REPORT NUMBER: AFML-TR-76-87	2. GOVT ACCESSION NO. / 3. RECIPIENT'S CATALOG NUMBER
4. TITLE (and Subtitle): AN ANALYTICAL METHOD FOR EVALUATING IMPACT DAMAGE ENERGY OF LAMINATED COMPOSITES.	5. TYPE OF REPORT & PERIOD COVERED: Final rept. May 1974 — May 1975
	6. PERFORMING ORG. REPORT NUMBER
7. AUTHOR(s): C. T. Sun	8. CONTRACT OR GRANT NUMBER(s): F33615-73-C-5112
9. PERFORMING ORGANIZATION NAME AND ADDRESS: Purdue University, School of Aeronautics & Astronautics, West Lafayette, Indiana 47907	10. PROGRAM ELEMENT, PROJECT, TASK AREA & WORK UNIT NUMBERS: 62102F, 73420210
11. CONTROLLING OFFICE NAME AND ADDRESS: Air Force Materials Laboratory (AFML/MBM), Air Force Wright Aeronautical Laboratories, Wright-Patterson AFB, Ohio 45433	12. REPORT DATE: June 1975; 13. NUMBER OF PAGES: 53
14. MONITORING AGENCY NAME & ADDRESS (if different from Controlling Office): 54p.	15. SECURITY CLASS. (of this report): Unclassified; 15a. DECLASSIFICATION/DOWNGRADING SCHEDULE

16. DISTRIBUTION STATEMENT (of this Report)

Approved for public release; distribution unlimited.

AF-7342 7342Ø2

17. DISTRIBUTION STATEMENT (of the abstract entered in Block 20, if different from Report)

18. SUPPLEMENTARY NOTES

19. KEY WORDS (Continue on reverse side if necessary and identify by block number)

Composite Materials
Impact
Dynamic Response
Laminated Composites
Finite Element
Hertzian Law
Damage Energy

20. ABSTRACT (Continue on reverse side if necessary and identify by block number)

A higher order beam finite element is developed for dynamic response of beams subjected to impact of elastic spheres. Hertzian law is used to evaluate the contact force. A step by step finite difference method is employed to integrate the time variable. The finite elements are first evaluated for homogeneous isotropic beams and excellent results are found. Impact of glass-epoxy laminates are then considered. The total energy imparted from the projectile to the laminate is computed and compared with experimental data. Good agreement is found. The present finite element procedure also allows one to separate the

over

DD FORM 1 JAN 73 1473 EDITION OF 1 NOV 65 IS OBSOLETE

UNCLASSIFIED

SECURITY CLASSIFICATION OF THIS PAGE (When Data Entered)

291850 LB

vibrational energy from the damage energy which is to be related to the residual strength of the composite after impact.

FOREWORD

In this report a higher order beam finite element is developed for dynamic response of beams subjected to impact of elastic spheres. The report was submitted by Purdue University, School of Aeronautics and Astronautics, West Lafayette, Indiana 47907, under Contract F33615-73-C-5112, Job Order 73420210, with the Air Force Materials Laboratory, Wright-Patterson Air Force Base, Ohio. C. T. Sun was the principal investigator and Dr. J. M. Whitney, AFML/MBM, was the project monitor. The report was released by the author, C. T. Sun, in June 1975. The period covered by the report was May 1974 to May 1975.

TABLE OF CONTENTS

LIST OF ILLUSTRATIONS

LIST OF TABLES

SECTION I

INTRODUCTION

In studying foreign object damage (FOD) of laminated fiber-reinforced composites, one often encounters extremely complex material as well as structural responses. First of all, the high velocity impact usually results in a substantial permanent deformation in the contact region. Secondly, the structural response is transient and it often requires a large number of vibrational modes to ensure an adequate description of the motion [1]. Consequently, most of the analytical work [2-3] is restricted to the elastic response of the laminate by neglecting the plastic deformation and by assuming that the contact force between the projectile and the laminate is known. Even with such simplifying assumptions, none is able to predict quantitatively the damage of the laminate due to impact.

In contrast to the small quantity of analytical work, experimental work is abundant [4]. Various tests have been performed in an effort to understand the failure mechanisms with the objective of developing practical protective measures. Although testing yields quantitative results, it is in general very restrictive and expensive. In view of the great variety of composites, a reliable analytical method is highly desirable in general applications, especially in optimal design.

The present work aims at developing a finite element method to determine the dynamic response as well as the energy that causes damages in the laminated composite due to impact of foreign objects. Such damage energy can be used to estimate the residual strength of the composite after impact. In this report, a higher order beam finite element is

presented complete with stiffness and consistent mass matrices. The finite element is evaluated by considering homogeneous and isotropic beams subjected to impact of elastic spheres for which analytical solutions are available. The elements are then employed to study beams of a glass-epoxy laminated composite. Solutions are compared with the experimental data obtained by Husman et al [5].

SECTION II

THE FINITE ELEMENT METHOD

We will consider symmetrically laminated cross-ply composites. Extension to unsymmetric laminates which exhibit bending-extension coupling can be easily carried out in the same manner. In the following, we will derive the stiffness matrix and the mass matrix for a homogeneous and isotropic beam element for which evaluation of the element efficiency will be made. The finite element for a symmetrically laminated cross-ply composite can be obtained from the isotropic one by using the appropriate stiffness coefficients. Bernoulli-Euler beam theory will be employed in modeling the finite element.

1. Finite Element Model for Isotropic Materials

The following power series for the shape function for the beam element in flexural deformation is taken:

$$v = a_1 + a_2x + a_3x^2 + a_4x^3 + a_5x^4 + a_6x^5 \qquad (1)$$

With this displacement function, there are three degrees of freedom at each nodal point, namely, the transverse displacement v_i, the rotation θ_i and the curvature κ_i (i=1,2). The displacement function can be expressed in terms of the six generalized nodal displacements.

Consider an elastic beam element of length L, cross-sectional area A, moment of inertia I and the elastic modulus given by E_b. The potential energy U and the kinetic energy T stored in this element are given by

$$U = \frac{E_b I}{2} \int_0^L \left(\frac{\partial^2 v}{\partial x^2}\right)^2 dx \tag{2}$$

and

$$T = \frac{\rho A}{2} \int_0^L (\dot{v})^2 dx \tag{3}$$

respectively. In Eq. (3), ρ is the mass density, and a dot represents the derivative with respect to time.

Corresponding to each degree of freedom at the nodal point, there is a generalized force. In this case we have Q_i, m_i and μ_i corresponding to v_i, θ_i and κ_i, respectively. The quantities Q_i and m_i are the usual shear force and moment, and μ_i is a hypermoment with the dimension lb-ft^2.

The potential energy of the generalized end forces for the element is

$$W_e = -\sum_{i=1}^{2} (Q_i v_i + m_i \theta_i + \mu_i \kappa_i) \tag{4}$$

Noting that the displacement function of the element is now expressed in terms of the six nodal displacement components, we can write U and T given by Eqs. (2) and (3) in terms of the six nodal displacement components. The equation of motion can be obtained by applying Hamilton's principle, i.e.,

$$\delta \int_{t_o}^{t_1} (U-T+W_e)dt=0 \tag{5}$$

with $\delta\Delta_i = 0$ at t_o and t_1.

The result is a system of six equations which can be written in matrix form as

$$\{F\} = [k]\{\Delta\} + [m]\{\ddot{\Delta}\} \tag{6}$$

where $\{F\}$ is the vector of the generalized forces associated with the nodal degrees of freedom $\{\Delta\}$; $[k]$ is the element stiffness matrix and $[m]$ is the element mass matrix. The explicit expression of Eq. (6) is given by

$$\begin{Bmatrix} Q_i \\ m_1 \\ \mu_1 \\ Q_2 \\ m_2 \\ \mu_2 \end{Bmatrix} = \frac{E_b I}{70L^3} \begin{bmatrix} 1200 & 600L & 30L^2 & -1200 & 600L & -30L^2 \\ & 384L^2 & 22L^3 & -600L & 216L^2 & -8L^3 \\ & & 6L^4 & -30L^2 & 8L^3 & L^4 \\ & & & 1200 & -600L & 30L^2 \\ & \text{sym.} & & & 384L^2 & -22L^3 \\ & & & & & 6L^4 \end{bmatrix} \begin{Bmatrix} v_1 \\ \theta_1 \\ \kappa_1 \\ v_2 \\ \theta_2 \\ \kappa_2 \end{Bmatrix}$$

$$+ \frac{\rho AL}{55440} \begin{bmatrix} 21720 & 3732L & 281L^2 & 6000 & -1812L & 181L^2 \\ & 832L^2 & 69L^2 & 1812L & -532L^2 & 52L^2 \\ & & 6L^4 & 181L^2 & -52L^3 & 5L^4 \\ & & & 21720 & -3732L & 281L^2 \\ & \text{sym.} & & & 832L^2 & -69L^3 \\ & & & & & 6L \end{bmatrix} \begin{Bmatrix} \ddot{v}_1 \\ \ddot{\theta}_1 \\ \ddot{\kappa}_1 \\ \ddot{v}_2 \\ \ddot{\theta}_2 \\ \ddot{\kappa}_2 \end{Bmatrix} \tag{7}$$

From the d'Alembert's dynamic condition of equilibrium and the condition of continuity at the nodal points, we obtain the system of

$$[H]\{\ddot{\Delta}\}_{t+\Delta t} = \{P\}_{t+\Delta t} - [K]\{b\}_t \tag{12}$$

where

$$[H] = [M] + \frac{\Delta t^2}{6}[K] \tag{13}$$

and

$$\{b\}_t = \{\Delta\}_t + \Delta t\{\dot{\Delta}\}_t + \frac{\Delta t^2}{3}\{\ddot{\Delta}\}_t \tag{14}$$

The solution for $\{\ddot{\Delta}\}_{t+\Delta t}$ can be obtained by inverting [H] in Eq. (12). However, a more efficient scheme is to solve Eq. (12) by the Gauss elimination procedure. With Eqs. (9) and (10), the current generalized displacement, velocity, and acceleration are obtained from those at the previous time. If appropriate initial conditions are given, the total response history can be generated by this step by step procedure.

We have also employed another finite difference procedure suggested by de Vogelaere [8] in some of the evaluative examples to be discussed later, and compared with the present method. It was found that these two methods were comparable.

It should be noted here that the choice of the time increment Δt is very critical in assuring the stability of the solution. According to the conclusion of Leech, Hsu and Mach [9], solution for Eq. (8) would be stable if

$$\Delta t \leq 2/\omega_m \tag{15}$$

equations of motion for the whole structure:

$$\{P\} = [K]\{\Delta\} + [M]\{\ddot{\Delta}\} \tag{8}$$

where $\{P\}$ indicates the external loads, and $[K]$ and $[M]$ are the assembled structural stiffness and mass matrices, respectively.

2. Integration of Time Variable

The solution for the equations of motion given by Eq. (8) can be solved by various methods [6]. A simple finite difference form proposed by Wilson and Clough [7] will be followed in the present analysis.

The essence of the procedure proposed by Ref. [7] resides in the assumption that the variation of the acceleration $\{\ddot{\Delta}\}$ is linear in the time interval Δt. Using the assumption, we have

$$\{\dot{\Delta}\}_{t+\Delta t} = \{\dot{\Delta}\}_t + \frac{\Delta t}{2}\{\ddot{\Delta}\}_t + \frac{\Delta t}{2}\{\ddot{\Delta}\}_{t+\Delta t} \tag{9}$$

and

$$\{\Delta\}_{t+\Delta t} = \{\Delta\}_t + \Delta t\{\dot{\Delta}\}_t + \frac{\Delta t^2}{3}\{\ddot{\Delta}\}_t + \frac{\Delta t^2}{6}\{\ddot{\Delta}\}_{t+\Delta t} \tag{10}$$

Substitution of equations (9) and (10) in (8) yields

$$\{P\}_{t+\Delta t} = [K](\{\Delta\}_t + \Delta t\{\dot{\Delta}\}_t + \frac{\Delta t^2}{3}\{\ddot{\Delta}\}_t + \frac{\Delta t^2}{6}\{\ddot{\Delta}\}_{t+\Delta_t}) + [M]\{\ddot{\Delta}\}_{t+\Delta t} \tag{11}$$

from which we obtain

$$[H]\{\ddot{\Delta}\}_{t+\Delta t} = \{P\}_{t+\Delta t} - [K]\{b\}_t \tag{12}$$

where

$$[H] = [M] + \frac{\Delta t^2}{6}[K] \tag{13}$$

and

$$\{b\}_t = \{\Delta\}_t + \Delta t\{\dot{\Delta}\}_t + \frac{\Delta t^2}{3}\{\ddot{\Delta}\}_t \tag{14}$$

The solution for $\{\ddot{\Delta}\}_{t+\Delta t}$ can be obtained by inverting [H] in Eq. (12). However, a more efficient scheme is to solve Eq. (12) by the Gauss elimination procedure. With Eqs. (9) and (10), the current generalized displacement, velocity, and acceleration are obtained from those at the previous time. If appropriate initial conditions are given, the total response history can be generated by this step by step procedure.

We have also employed another finite difference procedure suggested by de Vogelaere [8] in some of the evaluative examples to be discussed later, and compared with the present method. It was found that these two methods were comparable.

It should be noted here that the choice of the time increment Δt is very critical in assuring the stability of the solution. According to the conclusion of Leech, Hsu and Mach [9], solution for Eq. (8) would be stable if

$$\Delta t \leq 2/\omega_m \tag{15}$$

where ω_m is the highest natural frequency of the beam element. They also suggested that Δt should be no greater than one-sixth of the critical

value in order to obtain the fine high-frequency detail of the response. However, we have found that to insure the stability and to contain the higher frequencies of the higner order beam element model Δt should be no greater than one-tenth of the critical value. For nonlinear problem Δt should be even smaller.

3. Evaluative Example - Impulsive Loading

In order to test the efficiency of the present higher order element we consider a simply-supported beam of length L subjected to a sine pulse given by

$$P = P_o \sin \frac{\pi t}{\tau} \quad \text{for} \quad 0 \leq t \leq \tau \tag{16}$$

$$P = 0 \qquad \text{for} \quad t \geq \tau \tag{17}$$

The force is located at the center of the span. An analytical solution for the central deflection was obtained by Ref. [10] as

$$v_{L/2} = \frac{2P_o L^3}{\pi^4 E_b I} \sum_{i=1,3,5\ldots}^{\infty} \frac{1}{i^4} \left[\frac{4\tau^2}{4\tau^2 - T_i^2} \left(\sin \frac{\pi t}{\tau} - \frac{T_i}{2\tau} \sin \omega_i t\right)\right]$$

$$\text{for} \quad 0 \leq t \leq \tau \tag{18}$$

and

$$v_{L/2} = \frac{2P_o L^3}{\pi^4 E_b I} \sum_{i=1,3,5\ldots}^{\infty} \frac{1}{i^4} \left[\frac{4T_i \tau}{T_i^2 - 4\tau^2} \cos\left(\frac{\pi\tau}{T_i}\right) \sin \omega_i \left(t - \frac{\tau}{2}\right)\right]$$

$$\text{for} \quad t > \tau \tag{19}$$

where

$$T_i = \frac{2\pi}{\omega_i} = \frac{2L^2}{i^2 \pi} \sqrt{\frac{\rho A}{E_b I}} = \frac{T_1}{i^2}, \quad i=1,3,5\ldots \tag{20}$$

The following numerical values are taken:

P_o = 1000 lb, $\tau = 20 \times 10^{-6}$ second, $E_b = 30 \times 10^6$ psi and the beam is assumed to be $\frac{1}{2}$ - in x $\frac{1}{2}$ - in in cross-section and 30 in. in length.

The analytical results are obtained by retaining 1000 terms in Eqs. (18) and (19). A check shows that there is virtually no difference between a 250-term solution and a 1000-term solution. Accordingly, we can practically take the 1000-term solution as the exact solution.

Due to the symmetry, the higher order beam element model is generated for only one-half of the beam. The solution is carried out for N = 5, 10, 20, and 50, where N is the number of elements used for the half beam. For the purpose of comparison, the solution of the conventional 4 x 4 element [11] is also carried out. The central deflections at various times are shown in Table 1. It can be seen that the higher order element is superior to the 4 x 4 element. To manifest the far more superiority of the higher order element in obtaining stresses, the bending stress at the central span of the beam is carried out and shown in Table 2. It is easy to recognize that the accuracy of the 20-higher-order-element solution is about the same as that of the 50- 4 x 4 element. It takes CDC 6500 105 seconds central processor time for the former and 320 seconds for the latter. Thus, for the same degree of accuracy, the higher order element model uses about one-third the time as would be used by the 4 x 4 element model.

4. Elastic Impact

When subject to the impact of a mass, the beam receives an impulsive force which is the contact force between the mass and the beam. The

t (μ sec)	N = 5 Δt = 1.E-6 (sec)		N = 10 Δt = 1.E-6 (sec)		N = 20 Δt = 1.E-7 (sec)		N = 50 Δt = 5.E-8 (sec)		Exact Solution
	4 x 4	6 x 6	4 x 4	6 x 6	4 x 4	6 x 6	4 x 4	6 x 6	
1	8.062E-8	1.824E-7	1.602E-7	3.413E-7	3.128E-7	5.390E-7	5.326E-7	5.326#-7	5.328E-7
5	9.759E-6	2.139E-5	1.857E-5	2.896E-5	2.670E-5	2.868E-5	2.864E-5	2.868E-5	2.868E-5
10	7.039E-5	1.396E-4	1.198E-4	1.439E-4	1.433E-4	1.441E-4	1.440E-4	1.441E-4	1.441E-4
20	3.680E-4	5.162E-4	4.915E-4	4.974E-4	4.994E-4	4.984E-4	4.984E-4	4.984E-4	4.984E-4
30	6.612E-4	7.006E-4	7.418E-4	7.199E-4	7.209E-4	7.210E-4	7.210E-4	7.210E-4	7.210E-4
40	8.658E-4	8.876E-4	9.006E-4	8.847E-4	8.856E-4	8.861E-4	8.861E-4	8.861E-4	8.861E-4
50	1.019E-3	1.017E-3	1.012E-3	1.022E-3	1.024E-3	1.024E-3	1.024E-3	1.024E-3	1.024E-3
60	1.157E-3	1.158E-3	1.125E-3	1.143E-3	1.146E-3	1.146E-3	1.146E-3	1.146E-3	1.146E-3

Table 1. Central Deflection (inch) of the Beam of an Isotropic Material.

t (μ sec)	N = 5 Δt = 1.E-6 (sec)		N = 10 Δt = 1.E-6 (sec)		N = 20 Δt = 1.E-7 (sec)		N = 50 Δt = 5.E-8 (sec)		Exact Solution
	4 x 4	6 x 6	4 x 4	6 x 6	4 x 4	6 x 6	4 x 4	6 x 6	
1	-7.168E-1	-1.036E+1	-5.650E+0	-7.250E+1	-4.268E+1	-3.354E+2	-2.232E+2	-3.428E+2	-3.303E+2
5	-8.643E+1	-1.172E+3	-6.168E+2	-3.703E+3	-2.132E+3	-3.601E+3	-3.319E+3	-3.568E+3	-3.516E+3
10	-6.151E+2	-6.764E+3	-3.339E+3	-8.397E+3	-6.860E+3	-8.084E+3	-7.881E+3	-8.)70E+3	-7.997E+3
20	-3.005E+3	-1.198E+4	-8.084E+3	-7.471E+3	-8.397E+3	-7.968E+3	-7.498E+3	-7.387E+3	-7.388E+3
30	-4.590E+3	-2.279E+3	-6.555E+3	-4.775E+3	-4.946E+3	-4.757E+3	-4.780E+3	-4.750E+3	-4.750E+3
40	-4.658E+3	-4.548E+3	-4.966E+3	-3.913E+3	-3.850E+3	-3.850E+3	-3.846E+3	-3.837E+3	-3.835E+3
50	-4.153E+3	-2.133E+3	-3.178E+3	-3.314E+3	-3.316E+3	-3.295E+3	-3.328E+3	-3.305E+3	-3.304E+3
60	-3.8.8E+3	-4.181E+3	-2.371E+3	-2.846E+3	-3.011E+3	-2.987E+3	-2.983E+3	-2.937E+3	-2.935E+3

Table 2. Bending Stress (psi) at the Mid-span of the Beam of an Isotropic Material.

calculation of the contact force depends crucially on the local deformation at the contact region. The local deformation in turn is affected by the deflection of the beam. Timoshenko [12] initiated a basic approach in this area by combining the Hertzian contact force with the Bernoulli-Euler beam theory to analyze the transient dynamic response of a beam subjected to the impact of an elastic sphere. Several investigators later continued Timoshenko's work by either simplifying the computational procedure or employing the Timoshenko beam theory in the analysis [13-14]. Many experimental works have also been conducted [15-16]. In all the previous works, it was assumed that the vibration of the striking mass could be neglected. This assumption is supported by the result obtained by Rayleigh that very little vibration is induced in an oscillating system under the influence of forces of duration long in comparison with its natural periods.

Consider an elastic sphere striking the beam in the transverse direction. If the velocity of the sphere is not too high, the local deformation between the sphere and the beam can be regarded elastic, and, as a consequence, the Hertzian law of contact can be employed. Let F be the contact force and α be the relative approach, then the Hertzian law is given by

$$F = k_2 \alpha^{3/2} \tag{21}$$

where the contact point spring constant k_2 is given by

$$k_2 = \frac{4}{3} \frac{R_s^{1/2}}{\left(\frac{1-\nu_s^2}{E_s} + \frac{1-\nu_b^2}{E_b}\right)} \tag{22}$$

In Eq. (22), R_s is the radius of the sphere; ν_s, E_s and ν_b, E_b are the Poisson's ratios and the Young's moduli of the sphere and the beam, respectively. A derivation of Eq. (21) can be found in Ref. [17]. The relative approach α can be expressed in terms of the displacements of the mass and the beam as

$$\alpha = w - v(x_o) \tag{23}$$

where w is the displacement of the sphere measured from the position of the initial contact and $v(x_o)$ is the displacement of the beam at the point of contact $x = x_o$.

The equation of motion governing the mass is given by

$$m_s\ddot{w} = -k_2[w - v(x_o]^{3/2} \tag{24}$$

Thus, the motion of the sphere is nonlinearly coupled with that of the beam.

From Eq. (24) we have at time $t + \Delta t$

$$m_s\ddot{w}_{t+\Delta t} = -k_2[w_{t+\Delta t} - v_{t+\Delta t}(x_o)]^{3/2} \tag{25}$$

and

$$F_{t+\Delta t} = - m_s\ddot{w}_{t+\Delta t} \tag{26}$$

where $F_{t+\Delta t}$ denotes the contact force at $t+\Delta t$. As a first estimate, we assume that the values of $w_{t+\Delta t}$ and $v_{t+\Delta t}(x_o)$ can be approximated by

$$w_{t+\Delta t} = w_t + \Delta t\dot{w}_t + \frac{1}{2}\Delta t^2\ddot{w}_t \tag{27}$$

and

$$v_{t+\Delta t}(x_o) = v_t(x_o) + \Delta t \dot{v}_t(x_o) + \frac{1}{2}\Delta t^2 \ddot{v}_t(x_o) \qquad (28)$$

respectively. Substituting Eqs. (27) and (28) in Eq. (25), we obtain $\ddot{w}_{t+\Delta t}$ in terms of the known results at the previous time t. The contact force $F_{t+\Delta t}$ can subsequently be obtained from Eq. (26). Using this expression for the contact force in the established beam program, the displacement, velocity and acceleration at each nodal point can be computed.

However, more accurate values of $w_{t+\Delta t}$ and $v_{t+\Delta t}(x_o)$ can be obtained from the first approximate values. Using the formula given by Eq. (10), we can write

$$w_{t+\Delta t} = w_t + \Delta t\, \dot{w}_t + \frac{1}{3}\Delta t^2 \ddot{w}_t + \frac{1}{6}\Delta t^2\, \ddot{w}_{t+\Delta t} \qquad (29)$$

$$v_{t+\Delta t}(x_o) = v_t(x_o) + \Delta t\, \dot{v}_t(x_o) + \frac{1}{3}\Delta t^2 \ddot{v}_t(x_o) + \frac{1}{6}\Delta t^2 \ddot{v}_{t+\Delta t}(x_o) \qquad (30)$$

where $\ddot{w}_{t+\Delta t}$ and $\ddot{v}_{t+\Delta t}$ are obtained from the first round solution. Substituting Eqs. (29) and (30) in Eq. (25) and subsequently in Eq. (26) we obtain a modified contact force $F_{t+\Delta t}$, which, in turn, is used to yield a more accurate solution for the beam. Such iterative procedure can be carried on till the convergence criterion is met.

5. The Timoshenko Problem

In 1913, Timoshenko [12] investigated a 0.394 - in x 0.394 - in x 6.05 - in (1-cm x 1-cm x 15.35 cm) simply-supported beam subjected to the transverse impact of a steel ball of 0.394 in radius. The initial velocity of the sphere was 0.394 in/sec. The material constants taken were

$$\rho = 0.0089 \text{ slug/in}^3, \quad E_b = 31.3 \times 10^6 \text{ psi}, \quad \nu = 0.289 \tag{31}$$

In Timoshenko's solution, the resulting nonlinear integral equations were solved by a stepwise numerical integration procedure.

Due to the symmetry, only half of the beam is taken in the present analysis. The time step $\Delta t = 5 \times 10^{-8}$ second is used. The contact force history, the central deflection of the beam and the displacement of the sphere are computed till the contact ceases. The results are shown in Fig. 1. It is found that the present solutions agree very well with those obtained by Timoshenko. The rebound velocity of the sphere at the end of the contact is -0.1192 in/sec as compared with -0.1198 in/sec obtained by Timoshenko.

A similar problem can be found in Ref. [17], where a central transverse impact of a 1/2-in-diameter steel ball on a 1/2-in x 1/2-in x 30-in simply-supported steel beam was studied. The initial velocity of the ball was assumed to be 150 ft/sec. The material constants were

$$E_s = E_b = 30 \times 10^6 \text{ psi}, \quad \nu_b = 0.3, \quad \rho_s = \rho_b = 0.0088 \quad \text{slug/in}^3 \tag{32}$$

In Fig. 2, the contact force obtained by using 65 harmonics and time increment $\Delta t = 0.1\mu$ sec is reproduced from [17].

The solution according to the present finite element is obtained by employing 50 elements for half of the beam. The time step Δt is chosen to be 5×10^{-8} sec. The results are also shown in the figure for the sake of comparison. The agreement between these two solutions is excellent over a wide range of time. However, the maximum force obtained from the

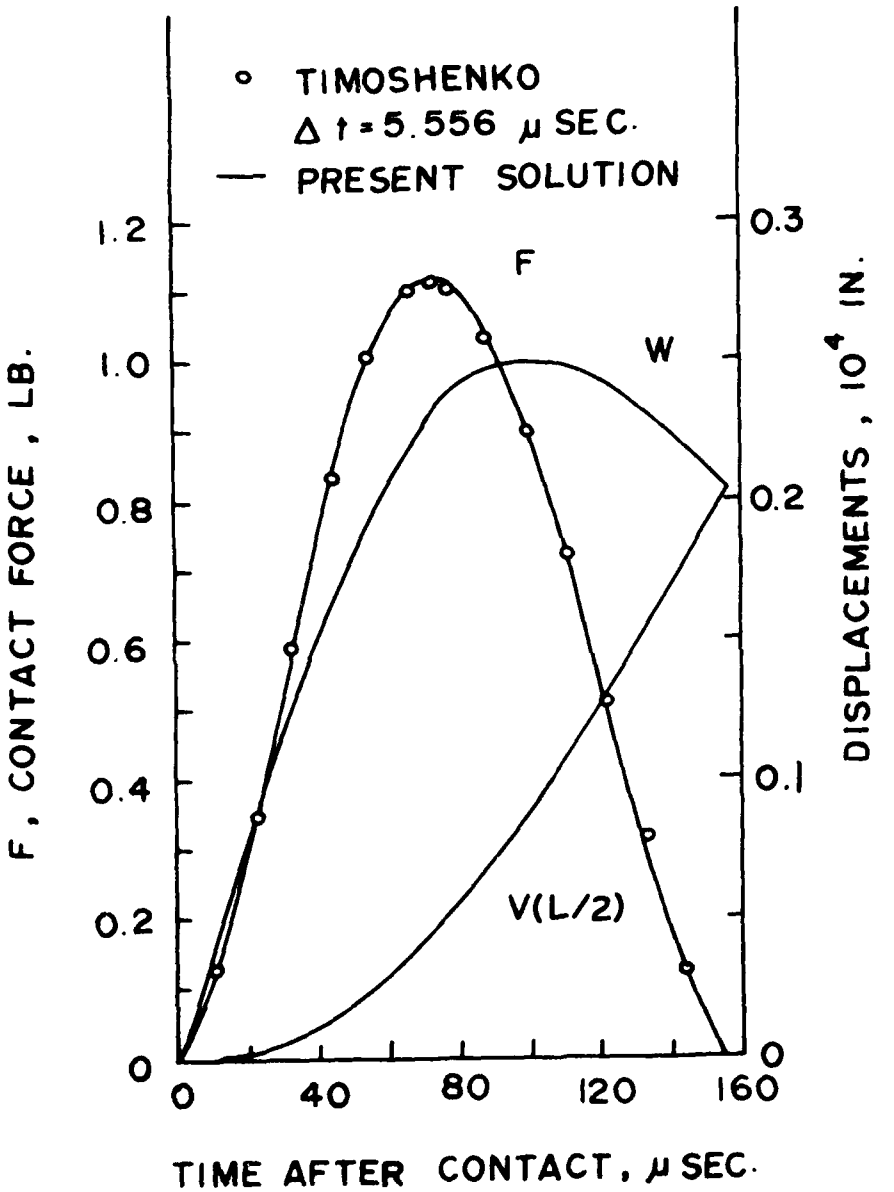

Fig. 1. Contact Force and Displacements of the Timoshenko Problem

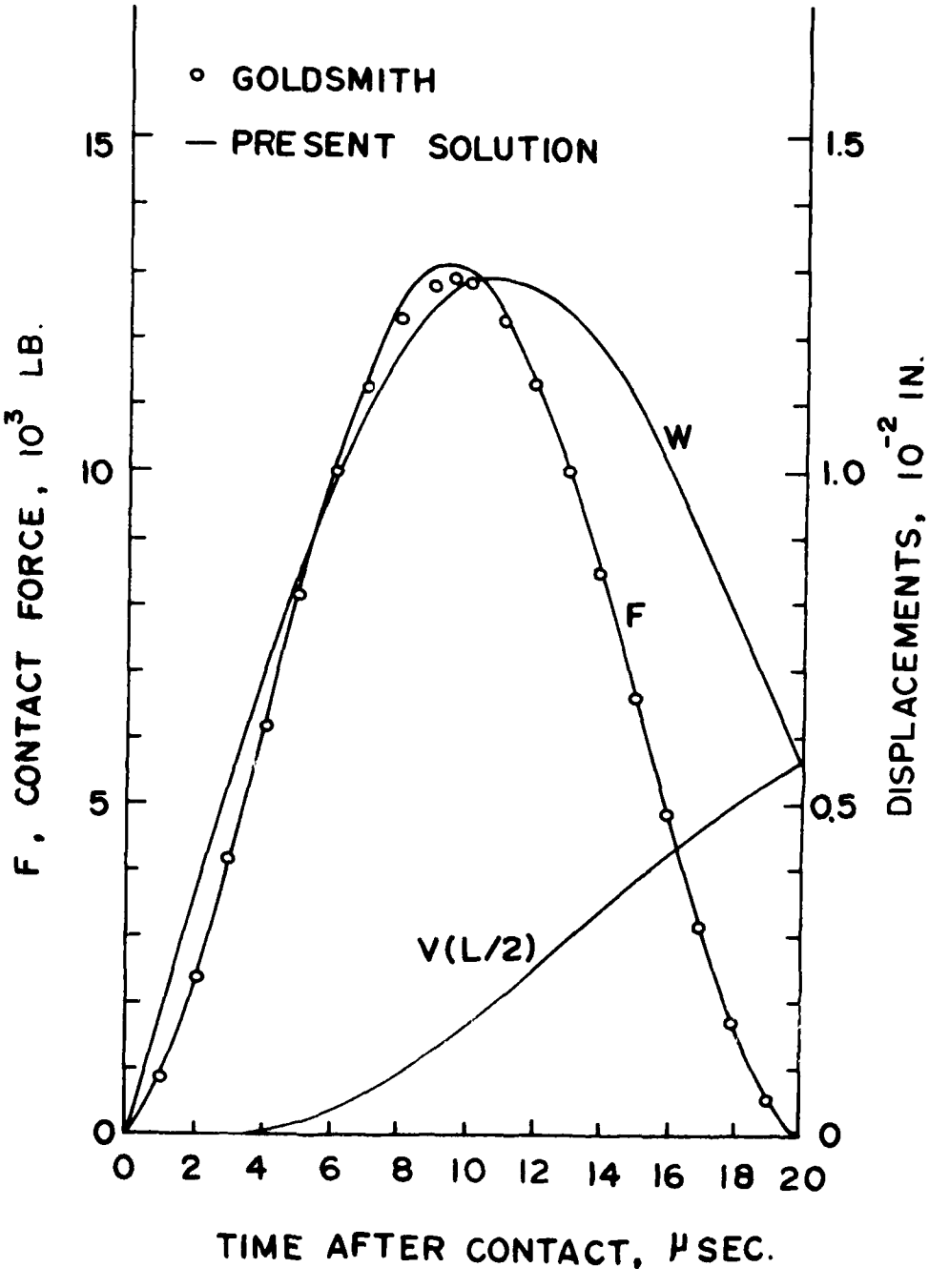

Fig. 2. Contact Force and Displacements of the Goldsmith Problem (with Δt = 0.1 μ sec and 65 Harmonics).

finite element method is about 2% higher than that obtained by [17]. It was revealed in [17] that if Δt was taken to be 2.735μ sec, then the maximum contact force would be reduced by about 9%. Thus, the foregoing discrepancy could have been reduced if smaller time steps were used by Goldsmith.

6. Impact with Permanent Indentation

Permanent craters can be generated even at relatively low impact speeds. According to Davis [18], a permanent crater formed when a 3/8-in-diameter steel sphere dropped from a height of 0.15 inch onto an armor plate which had a Brinell hardness 321. Therefore, it is more realistic to use a dynamic plastic force-indentation law instead of the Hertzian law of contact for the impact problem.

One of the approaches in obtaining the dynamic plastic force-indentation law was proposed by Barnhart and Goldsmith [19]. A sphere was dropped onto a steel block from heights of 1 to 13 feet. Initial velocity, rebound velocity and permanent crater depth were measured in each test. It was assumed that (1) the initial kinetic energy was completely transformed into the kinetic energy of rebound and the energy needed to form the permanent crater, (2) the rebound energy of the sphere was derived solely from the elastic strain energy stored equally in the sphere and the block during the indentation process, (3) the force law could be derived from the modified Hertzian law of contact: for indentation process,

$$F = N\alpha^n \qquad 0 \leq \alpha \leq \alpha_m \tag{33}$$

and for recovery process,

$$F = F_m\left[\frac{\alpha - \alpha_r}{\alpha_m - \alpha_r}\right]^q \qquad \alpha_m \geq \alpha \geq \alpha_r$$

where subscript m denoted the state of maximum relative approach, α_r was the permanent crater depth, q could be taken as 3/2 as in the Hertzian law, and N and n were determined from iterations of the following equations:

$$\frac{N}{n+1} \alpha_m^{n+1} = \frac{1}{2} m_s \dot{w}_o^2 - \frac{1}{4} m_s \dot{w}_f^2 \tag{35}$$

$$\frac{1}{4} m_s \dot{w}_f^2 = \frac{F_m}{q+1} (\alpha_m - \alpha_r) \tag{36}$$

In Eqs. (35) and (36), m_s was the mass of the sphere, w_o and w_f were the initial and rebound velocities of the sphere, respectively.

Using the force-deformation laws given by Eqs. (33) and (34), we consider a 1/2-in-diameter steel ball striking at the mid-span of a simply-supported beam. The steel beam has the dimensions 1/2-in x 1/2-in x 30-in and the material constants are given by Eq. (32). The initial velocity of the sphere is 150 ft/sec.

From Ref. [17] we found that the F-α law assumes the form

$$F = 1.29 \times 10^6 \alpha^{1.128} \qquad 0 \leq \alpha \leq \alpha_m \tag{37}$$

and from Ref. [16], we found that the average crater depth was $\alpha_r = 0.0123$ in. Thus, Eq. (34) takes the form

$$F = F_m \left[\frac{\alpha - 0.0123}{\alpha_m - 0.0123}\right]^{3/2} \qquad \alpha_m \geq \alpha \geq 0.0123 \tag{38}$$

The computer program developed earlier for the elastic impact can be readily extended to the present case. During the indentation period,

the Hertzian law of contact used in the elastic impact is simply replaced by Eq. (37), and during the recovery process Eq. (38) is used. It should be noted that F_m and α_m appearing in Eq. (38) can be obtained from the results for the identation process when the maximum relative approach is reached.

The results obtained based on 50 finite elements and $\Delta t = 0.05\mu$ second are shown in Fig. 3. The contact force given by Goldsmith [17] is also plotted for comparison. Again, the agreement is good over the whole period except in the vicinity of the maximum contact force. This discrepancy can be explained in the same manner as in the elastic case described in Section II.5.

7. Finite Element for a Laminated Composite

If the Bernoulli-Euler beam theory is employed to model the symmetric cross-ply laminated composite, then its stiffness matrix can be obtained from Equation (7) by replacing $E_b I$ by the bending stiffness of the laminate given by

$$D_b = \int_{-h/2}^{h/2} bE_i \, z^2 \, dz \tag{39}$$

where b is the width of beam, E_i is the Young's modulus of the ith lamina in the x-direction, z is the thickness coordinate, and h is the thickness of beam. It is noted that $E_i = E_L$ (the longitudinal Young's modulus) if the fibers direction in the ith lamina is parallel to the x-axis. If the fibers are transverse to x-axis, then $E_i = E_T$ (the transverse Young's modulus).

The indentation law for an elastic isotropic sphere on the laminated composite is assumed to have the same expression given by Eq. (21). Such

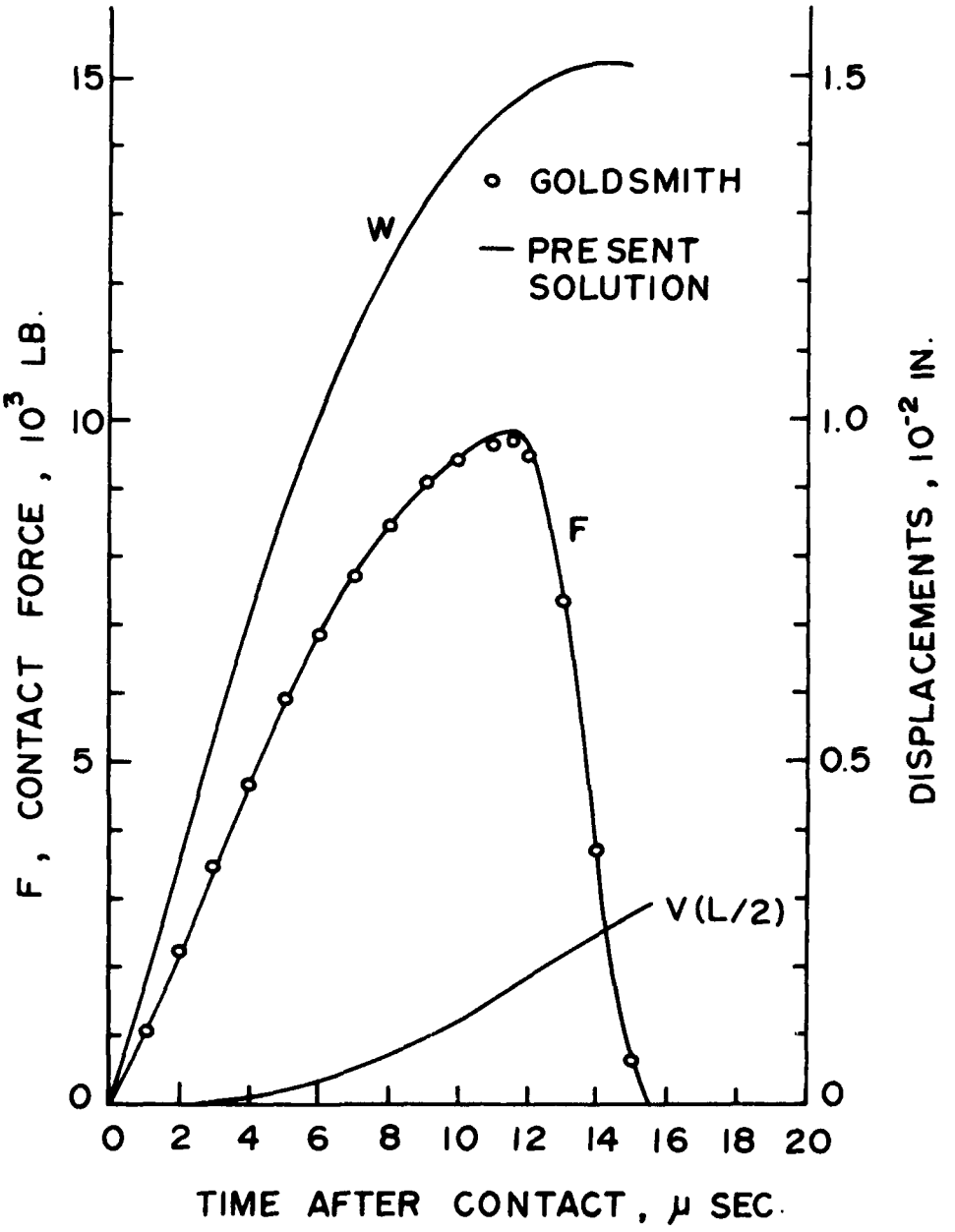

Fig. 3. Contact Force and Displacements of a Simply-Supported Beam with Permanent Indentations after Impact.

formula was found to be valid by Willis [22] for a rigid sphere pressed on a transversely isotropic halfspace. In the present work, the spring constant is taken as

$$k_2 = \frac{4}{3} \frac{R_s^{1/2}}{\left(\frac{1-\nu_s^2}{E_s} + \frac{1}{E_T}\right)} \tag{40}$$

SECTION III

IMPACT RESPONSE OF COMPOSITE MATERIALS

We now proceed to use the finite element and the modified Hertzian contact law to study the dynamic response of a laminated beam and the energy imparted from the striking mass to the beam. It is clear that our main objective is to predict the work done by the projectile on the beam. It should be noted that the total amount of energy of the mass is, in general, absorbed in two forms, namely the vibrational energy stored in the form of vibration of the laminate and the energy dissipated in the contact zone. For a hard projectile, damage generally occurs in the contact area and the vibrational energy which, in this case, does little damage to the beam will be damped out. In view of this, it is desirable to separate these two types of energies received from the striking mass and relate the "damage energy" to the reduction of strength of the laminate.

1. The Elastic Response.

Consider cantilever beams of laminated composites subjected to the impact of a mass at the midpoint of the length. By using the finite element method described in Section II, the entire response history of the beam and mass can be obtained. In Figs. 4-14, results for various approach velocities are presented for Scotch ply/1002 laminated composites. The elastic constants are

$$E_L = 5.7 \times 10^6 \text{ psi}, \; E_T = 1.7 \times 10^6 \text{ psi}, \; \rho = 0.00202 \text{ slug/in}^3$$

The projectile is a steel ball of diameter 0.177 in. Twenty-four elements are used with $\Delta t = 0.1$ μ second. The same dimensions of

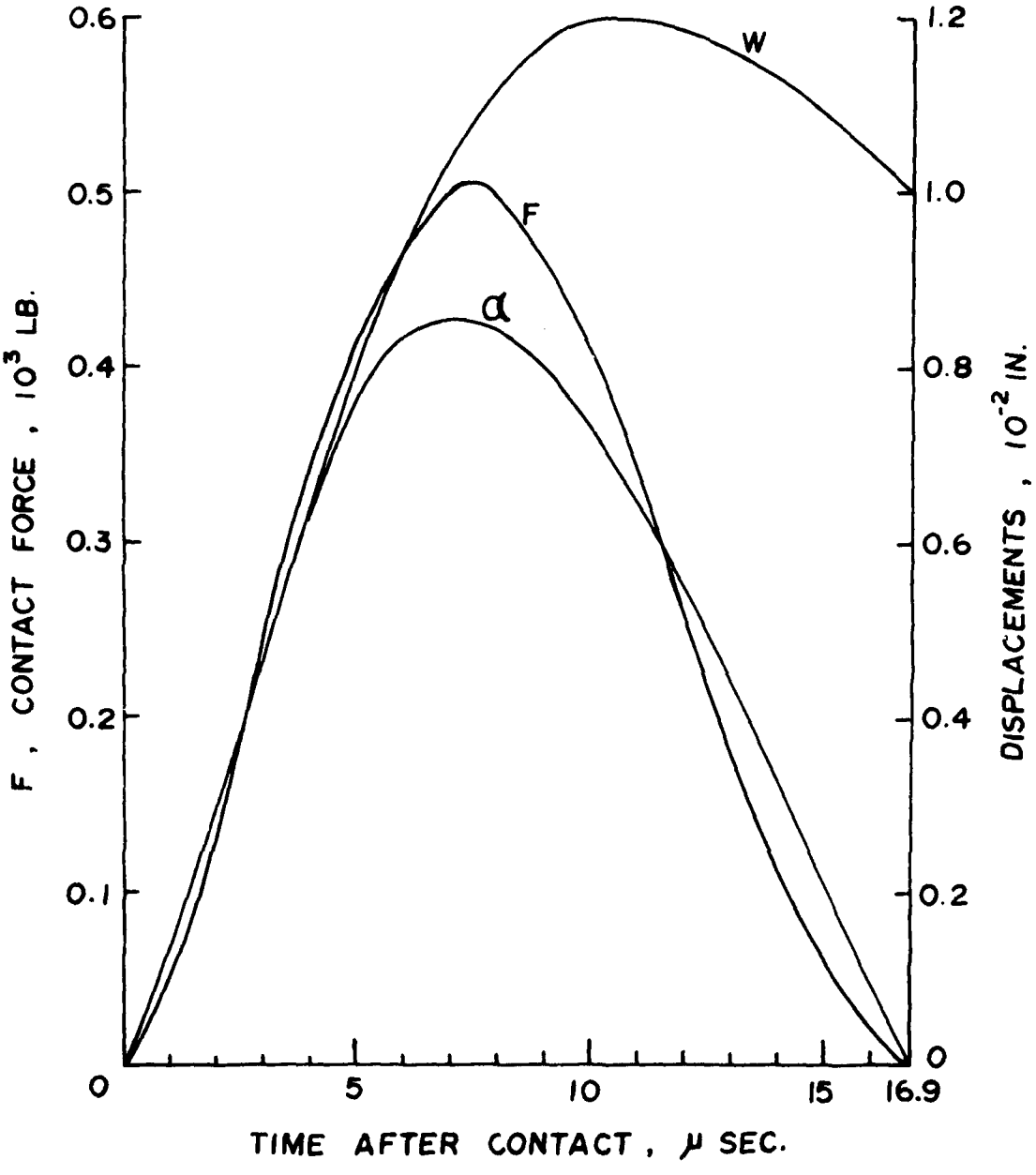

Fig. 4. Impact Response History of the Laminated Cantilever of 0.5" x 0.097" x 6" for Approach Velocity of 150 fps.

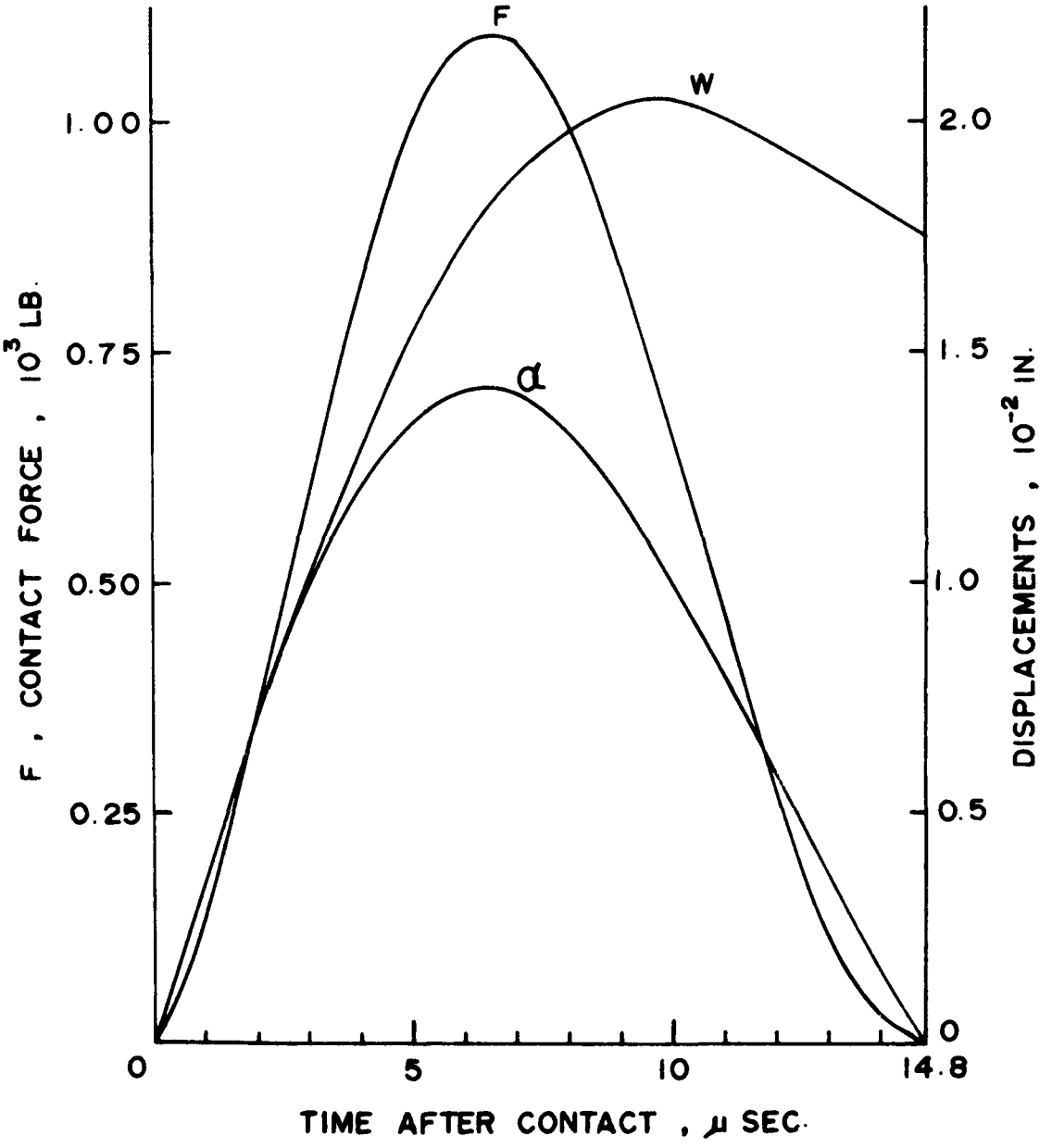

Fig. 5. Impact Response History of the Laminated Cantilever of 0.5" x 0.097" x 6" for Approach Velocity 290 fps.

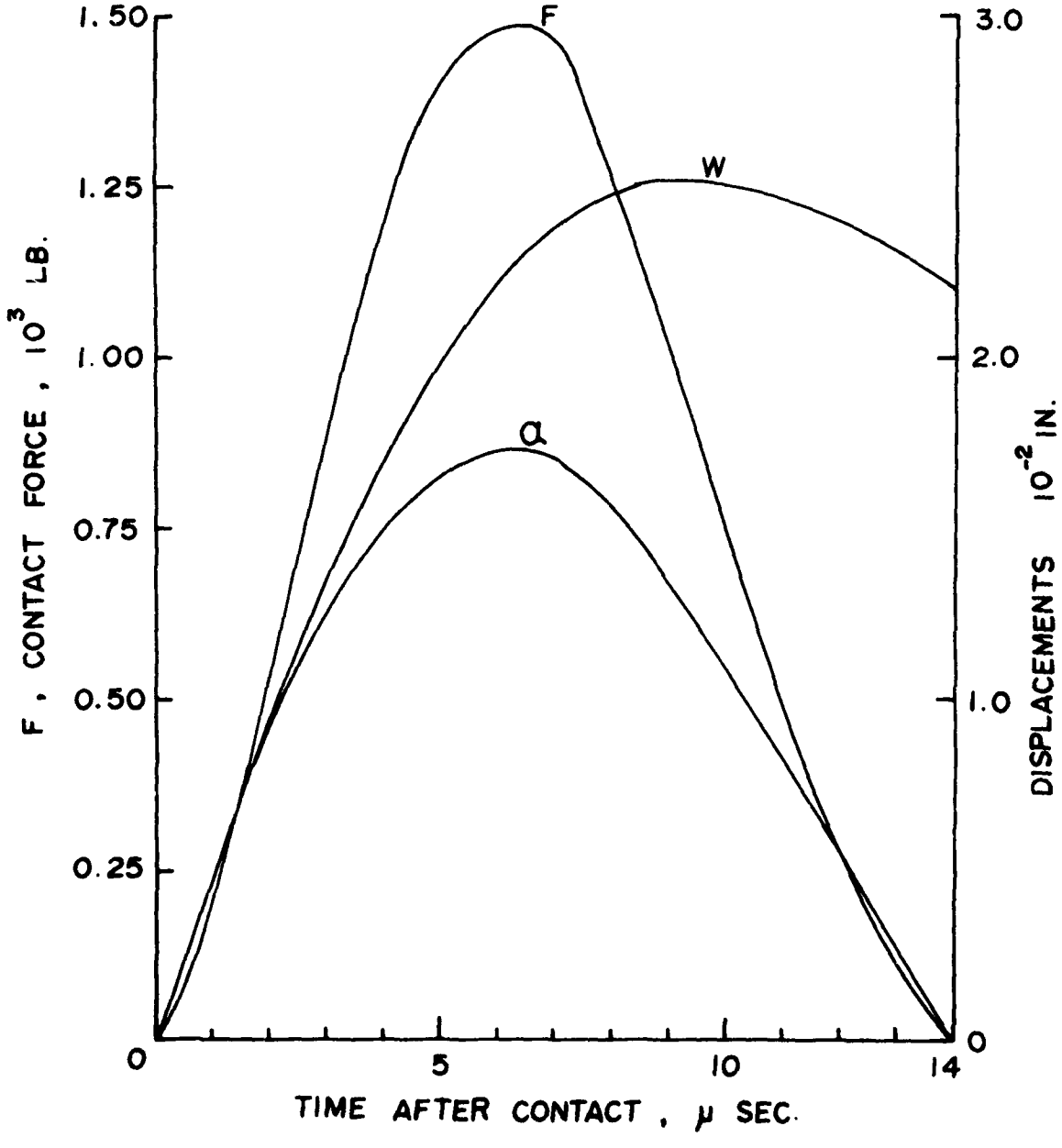

Fig. 6. Impact Response History of the Laminated Cantilever of 0.5" x 0.097" x 6" for Approach Velocity 377 fps.

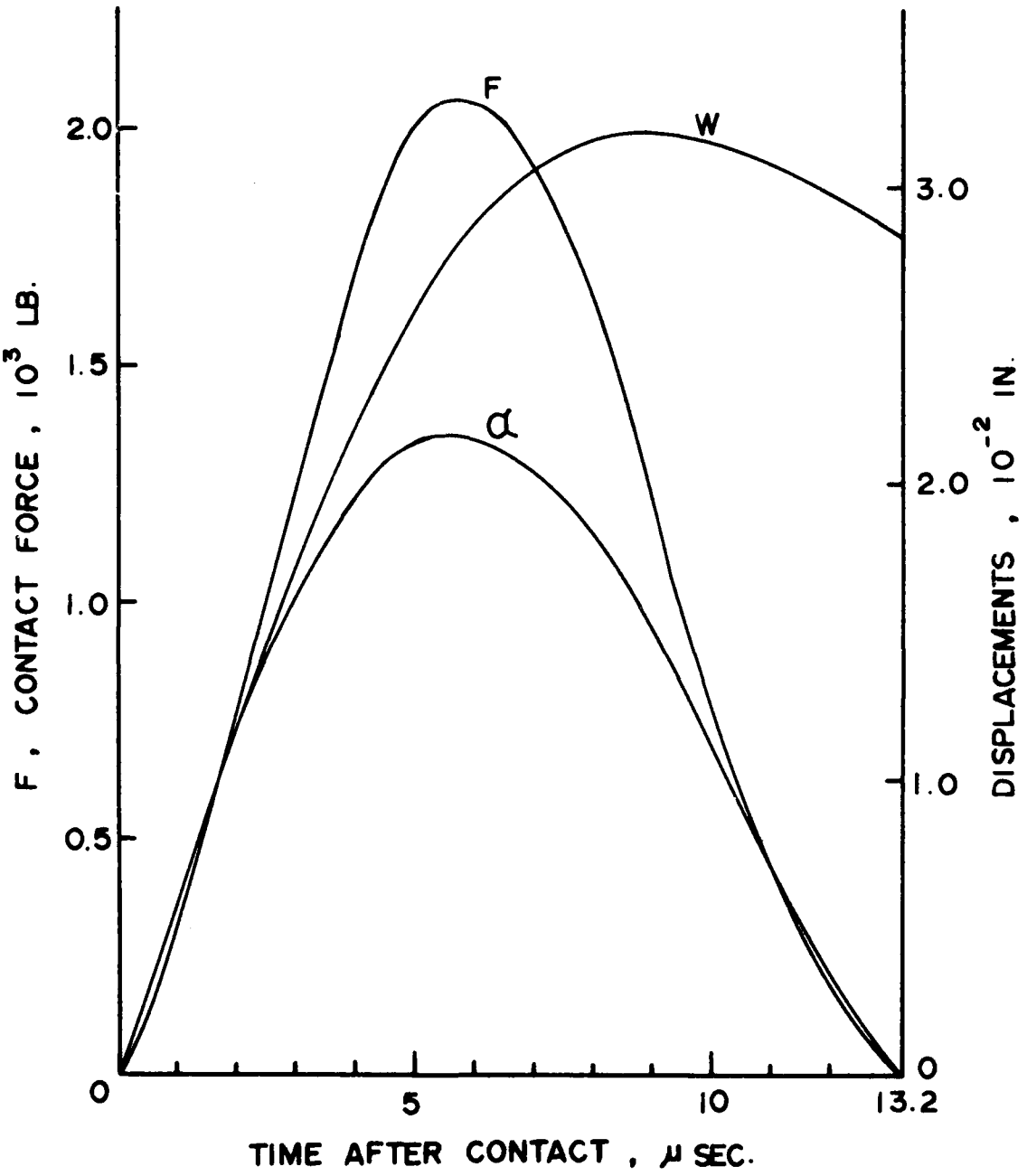

Fig. 7. Impact Response History of the Laminated Cantilever of 0.5" x 0.097" x 6" for Approach Velocity 500 fps.

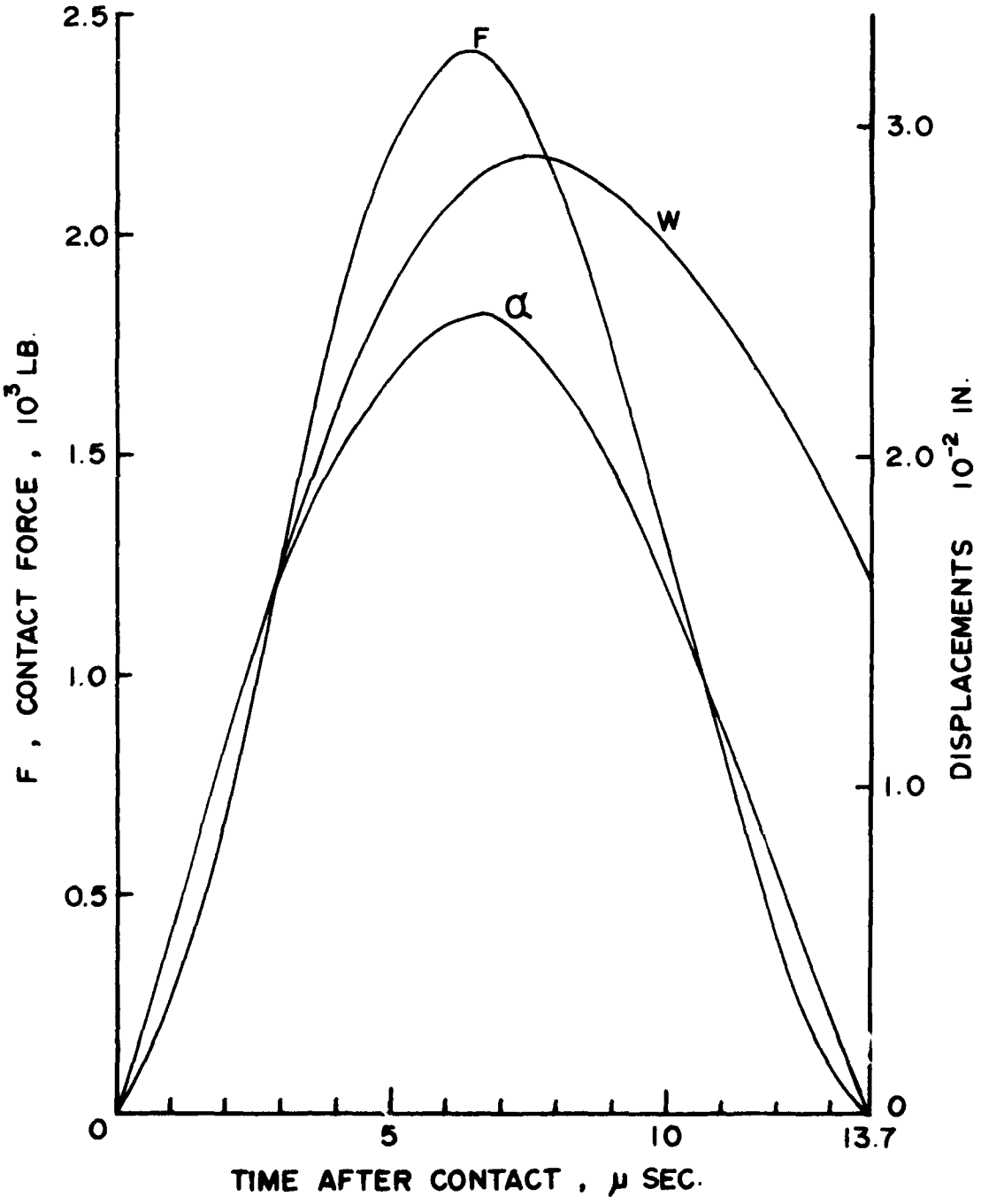

Fig. 8. Impact Response History of the Laminated Cantilever of 1" x 0.102" x 6" for Approach Velocity 483 fps.

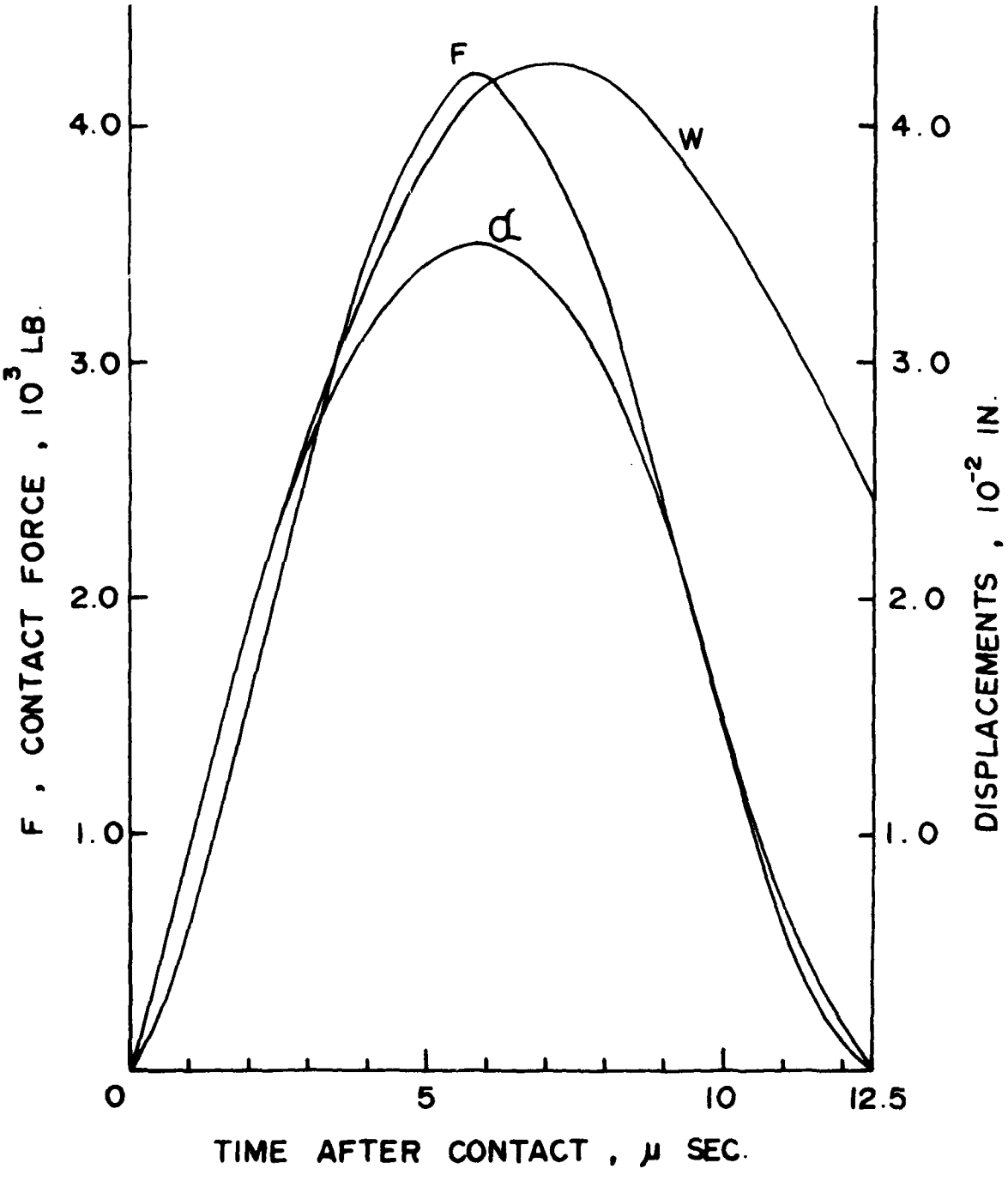

Fig. 9. Impact Response History of the Laminated Cantilever of 1" x 0.102" x 6" for Approach Velocity 775 fps.

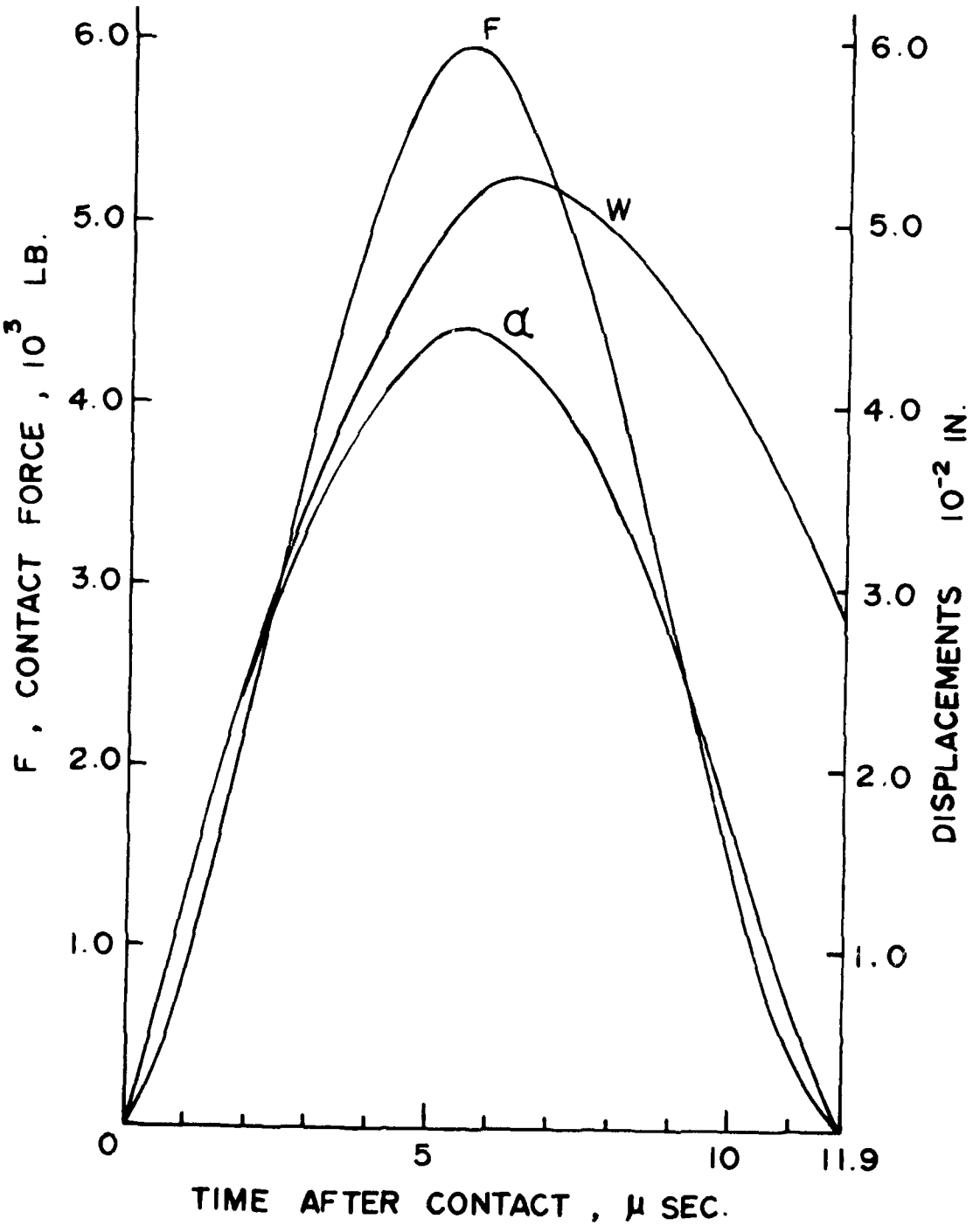

Fig. 10. Impact Response History of the Laminated Cantilever of 1" x 0.105" x 6" for Approach Velocity 1013 fps.

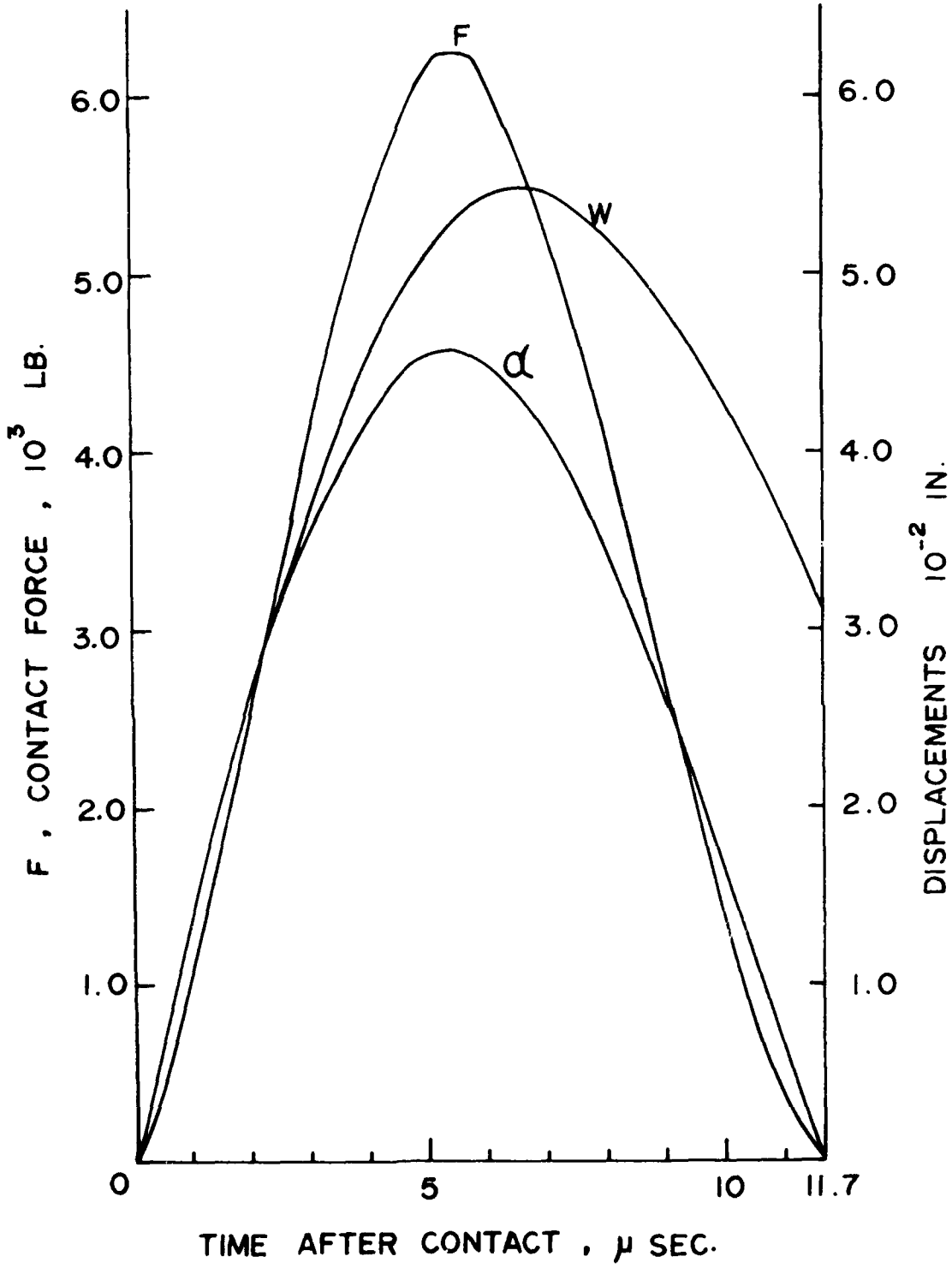

Fig. 11. Impact Response History of the Laminated Cantilever of 1" x 0.107" x 6" for Approach Velocity 1067 fps.

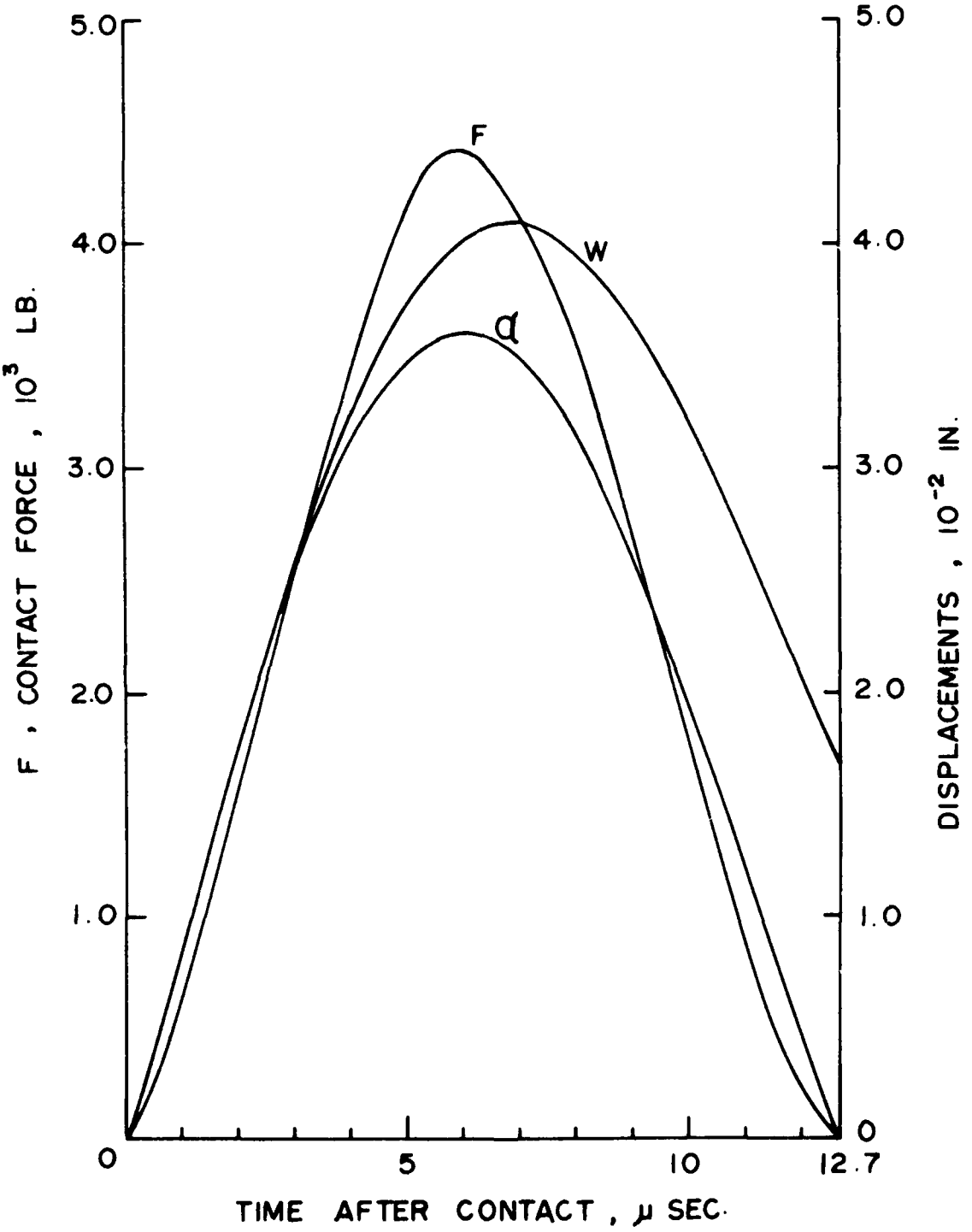

Fig. 12. Impact Response History of the Laminated Cantilever of 1.5" x 0.104" x 6" for Approach Velocity 754 fps.

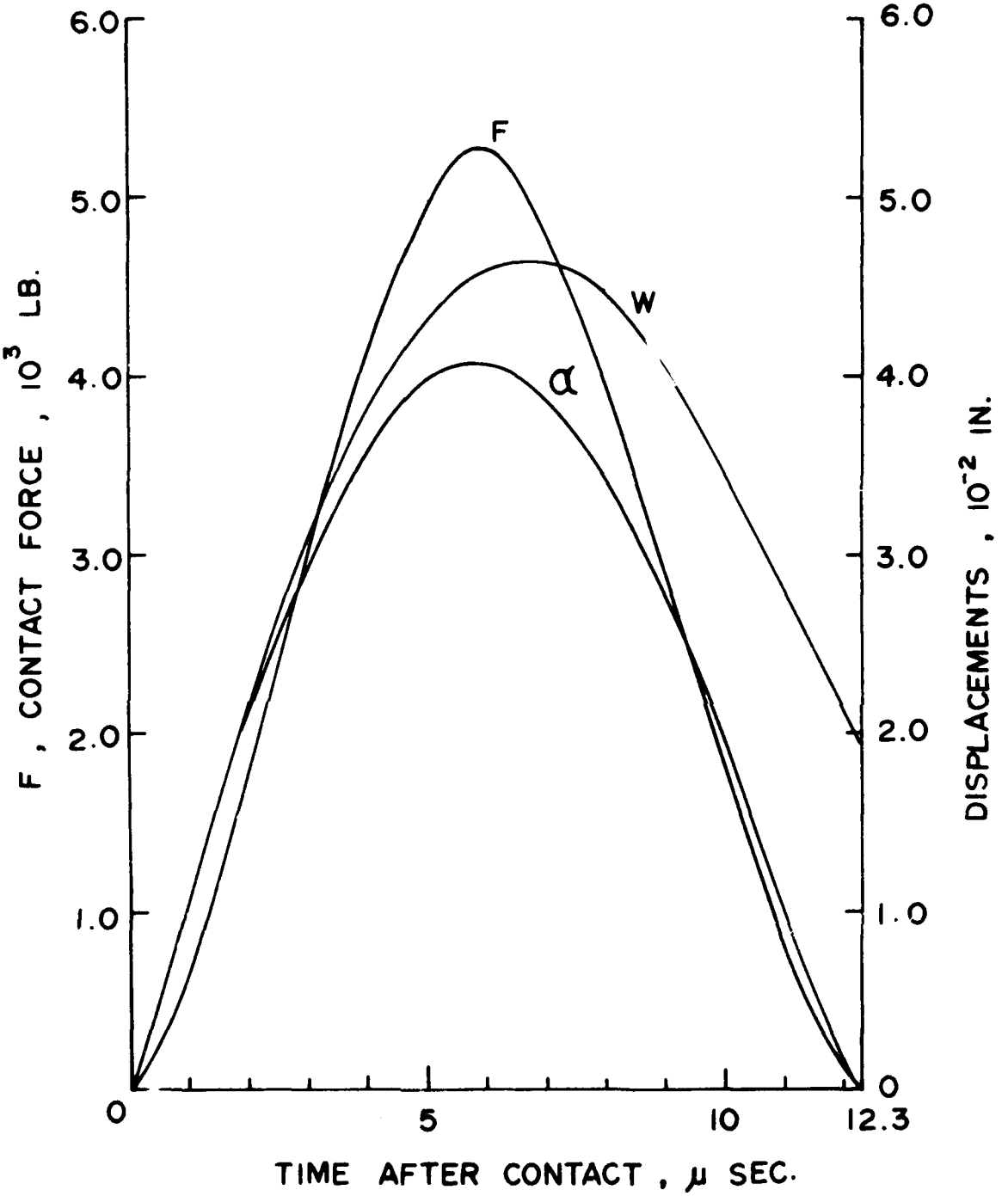

Fig. 13. Impact Response History of the Laminated Cantilever of 1.5" x 0.103" x 6" for Approach Velocity 880 fps.

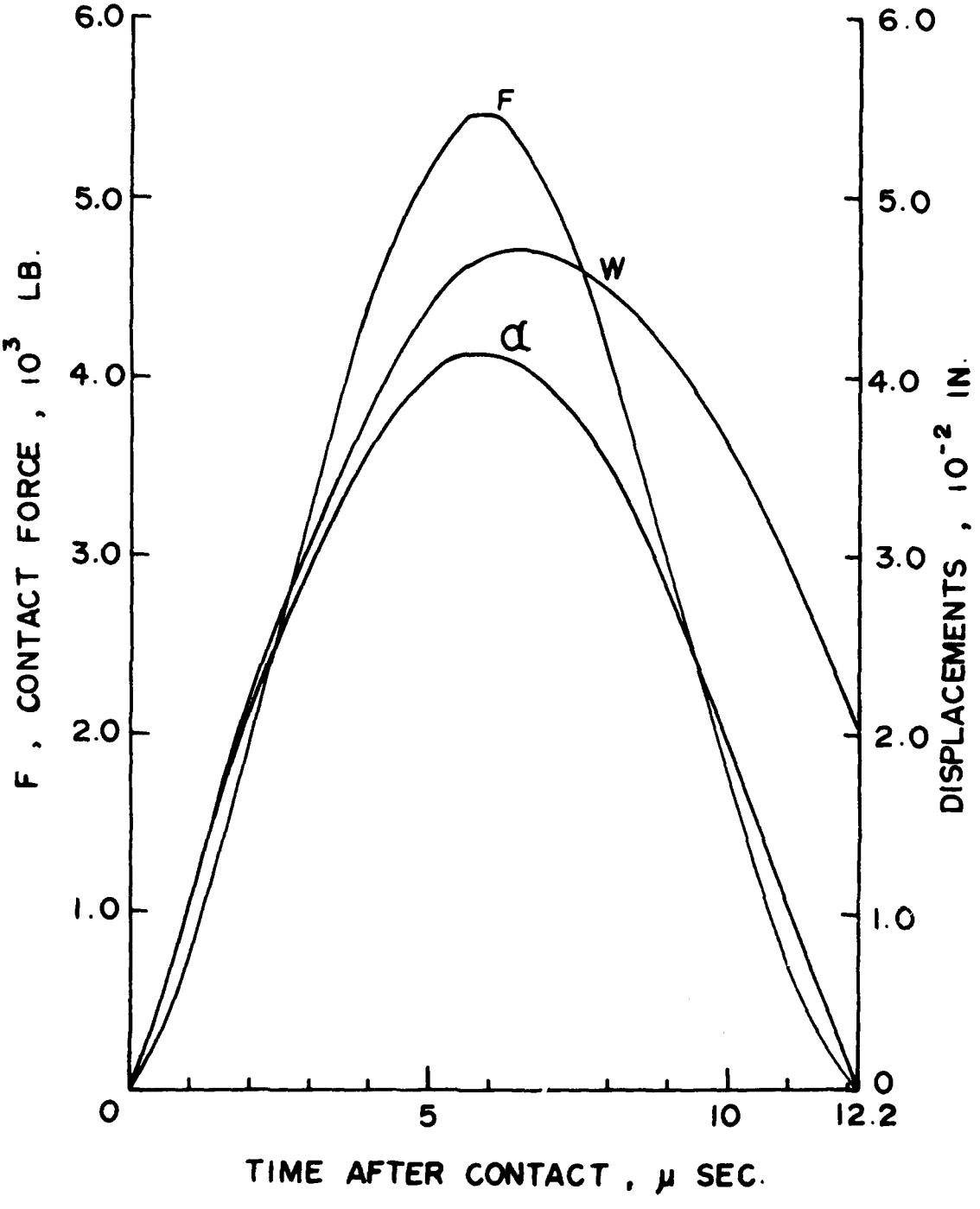

Fig. 14. Impact Response History of the Laminated Cantilever of 1.5" x 0.104" x 6" for Approach Velocity 904 fps.

specimens and materials were also used by Husman et al in their experiments [5].

The energy imparted from the sphere to the laminate during the period of contact can be evaluated in several ways. We can either compare the initial and rebound velocities of the mass or the contact force and displacement histories. We have

$$KE = \frac{1}{2} m_s(\dot{w}_o^2 - \dot{w}_f^2) \tag{42}$$

or

$$KE = \int_o^{w_f} F \, dw \tag{43}$$

where w_f is the displacement of the mass when the contact ceases.

Of course, one cannot expect these elastic solutions to compare favorably with the experimental results. The reason is obvious: The inelastic response in the contact zone is too substantial to neglect.

2. Estimate of the Imparted Energy

The finite element procedure can be used for any kind of inelastic contact law. In the future, if such laws are established, the finite element solution should be able to yield more accurate response histories. However, for the FOD of composites problems, we are mainly concerned with the energy absorbed by the laminate rather than its dynamic response history. With this in mind, we are able to utilize the special material properties of the fiber-reinforced composite to estimate this energy with surprisingly accurate results.

From all the available experimental data, the stress-strain relations of fiber-composite composites behave almost linearly up to failure. Only

the longitudinal shear exhibits somewhat nonlinear behavior. Since in the present consideration the longitudinal shear deformation is negligible, the linear relations are valid in the loading stage. Only when the indentation reaches its maximum depth and starts to recover, the linearly elastic relations should be subject to reexamination. If we assume that the elastic recovery of deformation is negligible as in rigid plasticity, then the relation of the contact force and the indentation α can be represented by the curve shown in Fig. 15. In other words, the contact force will drop to zero after it passes the maximum value of α in the elastic solution; and in the subsequent time, the mass does no work to the beam. The total amount of work done by the projectile becomes

$$KE_T = \int_0^{w_{max}} F \, dw \tag{44}$$

where w_{max} is the displacement of the sphere at $F = F_{max}$. It should be noted that w_{max} is not the maximum value of w.

Using Eq. (44), we compute KE_T and tabulate the results in Table 3. Our analytical results are excellent as compared with the experimental results obtained by Husman et al [5].

3. The Damage Energy

Since not all the work done by the projectile can be converted to energy dissipated in the damage zone, the total imparted energy KE_T cannot be used to account for the amount of damage received by the laminate. A more pertinent quantity is the damage energy defined by

$$KE_D = \int_0^{\alpha_{max}} F \, d\alpha \tag{45}$$

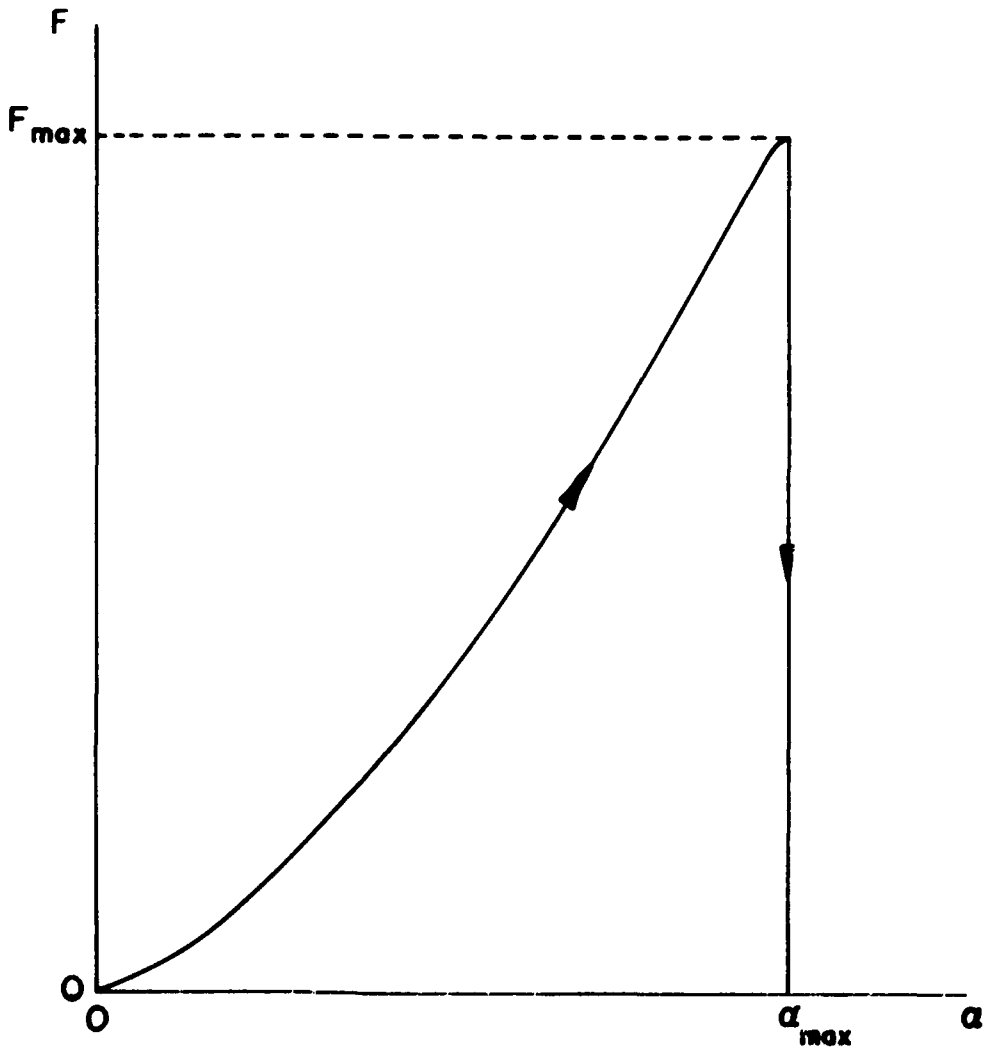

Fig. 15. Assumed Loading and Unloading Path with Permanent Indentation.

Dimension of Specimen (in)	Approach Velocity (fps)	KE_T (ft-lbs)	KE_T^* (ft-lbs)	KE_D (ft-lbs)	KE_D^* (ft-lbs)	Experiment $K E_T$ (ft-lbs)
0.5x0.097x6	150	0.222	0.233	0.143	0.141	0.194
0.5x0.097x6	290	0.814	0.851	0.519	0.515	0.836
0.5x0.097x6	377	1.353	1.414	0.862	0.854	1.505
0.5x0.097x6	500	2.38	2.45	1.49	1.48	2.79
1.0x0.102x6	483	2.61	2.66	1.95	1.94	2.66
1.0x0.102x6	775	6.70	6.85	4.93	4.91	7.16
1.0x0.105x6	1013	11.62	11.75	8.75	8.72	12.30
1.0x0.107x6	1067	12.62	12.84	9.47	9.44	13.70
1.5x0.104x6	754	6.55	6.62	5.28	5.26	6.78
1.5x0.103x6	880	8.89	9.00	7.14	7.11	9.30
1.5x0.104x6	904	9.43	9.51	7.56	7.53	9.80

Table 3. Total Imparted and Damage Energies of Laminated Beams of a Glass-Epoxy Composite.

The rest of the work done is stored in the form of vibrational energy given by

$$KE_V = KE_T - KE_D = \int_0^{v_{max}} F \, dv \tag{46}$$

where v_{max} is the displacement of the beam at the contact point when $F = F_{max}$. The results are also shown in Table 3.

SECTION IV

DISCUSSIONS AND RECOMMENDATIONS

Damages of turbine fan blades of advanced composites due to impact of foreign objects are to be related to their residual strengths. In this report, an effort is made to develop a finite element method for determining the amount of energy that causes damages in the area of impact. The model is derived based upon linear stress-strain relations and a modified Hertzian contact law. The results are excellent in comparison with existing experimental data for glass-epoxy laminated composites. With this analytical procedure, more general type of laminates can be considered and optimal design with respect to impact strength of blades is feasible. The greatest advantage of this model resides in its simplicity and without using inelastic material behaviors which have been deemed necessary in solving FOD problems.

However, in adopting this model, several restrictions must be imposed. First, the blade can only be modeled as a beam. Second, the projectile should be relatively hard so that the damage zone is confined in the vicinity of the contact region. The applications are more suitable for impact of hailstones and gravels rather than birds. The response of blades to impact of birds is substantially different from that of the hard objects. A soft body such as a bird usually leads to a longer contact time and is able to produce larger amplitude stress waves in the blade. Such waves with high stress levels could produce failure of the blade at distant regions such as the root, and the local damage might be less significant. Furthermore, the bird itself could absorb a substantial

amount of energy during its destruction. In using finite element for soft body impact, the finite element for the blade must be modeled to account for large deflection and the soft body be modeled by viscoplastic finite elements. This part of the work is underway and will be reported in the future.

In order to model more realistically an actual turbine fan blade, a plate finite element should be used. The two-dimensional plate element can describe the twist geometry of the fan blade by using the usual co-ordinate transformation for finite elements.

Finally, although it is of less practical interest, the elastic unloading can be incorporated in the present analysis in a crude manner. As mentioned previously, unloading occurs after the contact force passes its maximum value as shown schematically in Fig. 16. Exact unloading path is unclear at this stage. We propose to estimate the elastic strain to be recovered as

$$\varepsilon_e = Y/E_T \tag{47}$$

where Y is the transverse strength of the fiber-reinforced composite. The total recovery displacement at the is given by

$$\alpha_e = \frac{1}{2} h \varepsilon_e \tag{48}$$

The one-half factor is used to account for the fact that the compressive strain over the thickness of beam is not uniform and the average value is taken. With this consideration, the projectile remains in contact with the beam till the value of α passes α_{max} and reaches $\alpha_{max}-\alpha_e$. Thus, the

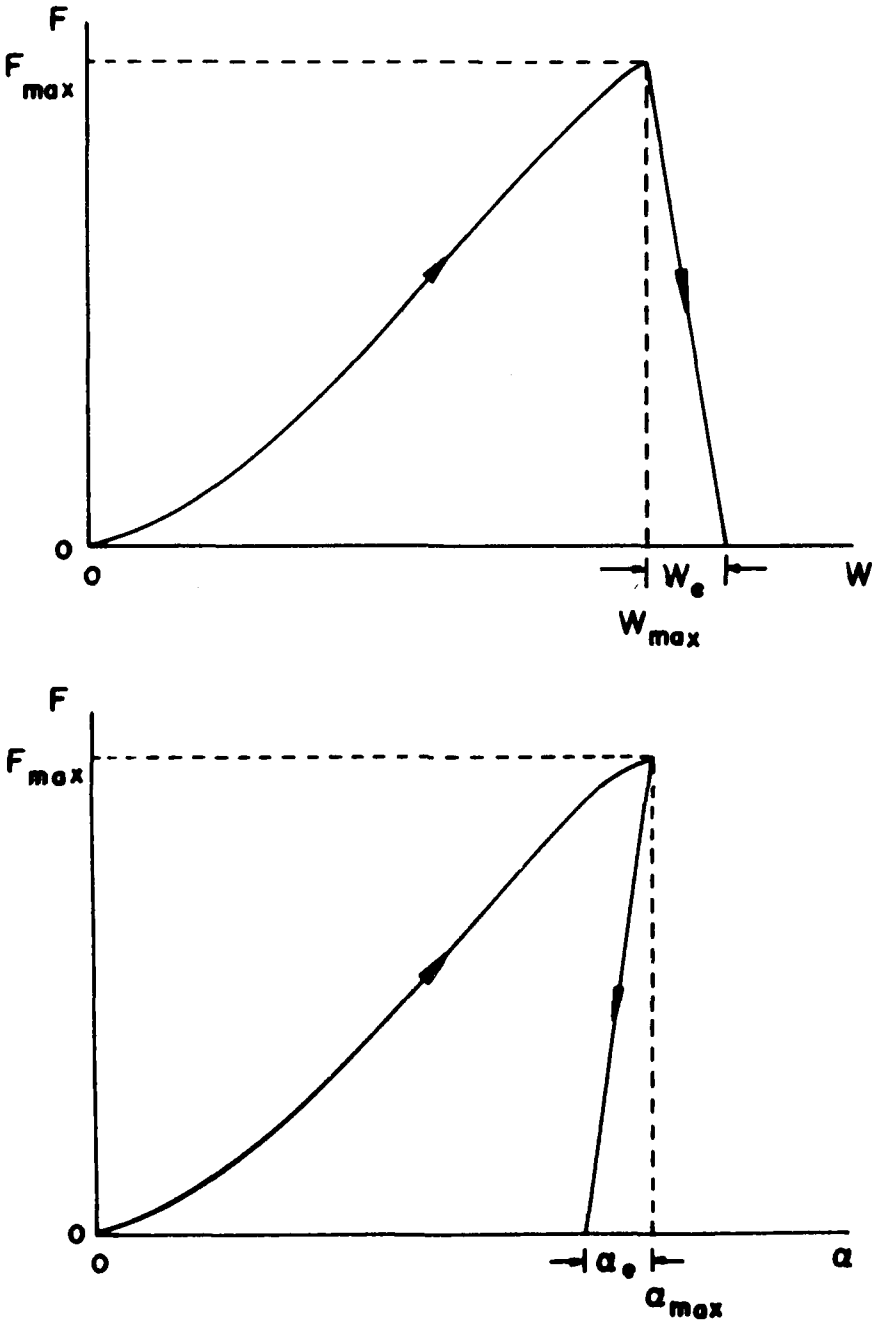

Fig. 16. Contact Force with Elastic Recovery.

total work done by the projectile becomes

$$KE_T^* = \int_0^{w_{max}} F\, dw + \frac{1}{2} F_{max}\, w_e \tag{49}$$

where w_e is the displacement of the projectile corresponding to $\alpha = \alpha_{max} - \alpha_e$ after passing $\alpha = \alpha_{max}$. It is noted that one-half is added to the second term to approximately account for the fact that the contact force should drop from F_{max} to zero in the region of unloading. The damage energy KE_D can be corrected in a similar manner. We have

$$KE_D^* = KE_D - \frac{1}{2} F_{max}\, \alpha_e \tag{50}$$

In the calculation, we choose $Y = 4 \times 10^3$ psi. Both KE_T^* and KE_D^* are presented in Table 3. Some improvement is noted.

REFERENCES

1. C. T. Sun, and S. Chattopadhyay, "Dynamic Response of Anisotropic Laminated Plates Under Initial Stress to Impact of a Mass," AFML-TR-74-258, December, 1974. Also to appear in Journal of Applied Mechanics.

2. F. C. Moon, "Theoretical Analysis of Impact in Composite Plates," NASA CR-121110.

3. J. T. Kubo and R. B. Nelson, "Analysis of Impact Stresses in Composite Plates," Foreign Object Impact Damage to Composites, ASTM STP 568, pp. 228-244, 1975.

4. Foreign Object Impact Damage to Composites, ASTM STP 568, 1975.

5. G. E. Husman, J. M. Whitney, and J. C. Halpin, "Residual Strength Characterization of Laminated Composite Subjected to Impact Loading," Foreign Object Impact Damage to Composites, ASTM STP 568, pp. 92-113, 1975.

6. O. C. Zienkiewicz, The Finite Element Method in Engineering Science. McGraw-Hill, New York, 1971.

7. E. L. Wilson and R. W. Clough, "Dynamic Response by Step by Step Matrix Analysis," Symp. on Use of Computers in Civil Eng., Lisbon, October 1962.

8. R. de Vogelaere, "A Method for the Numerical Integration of Differential Equations of Second-Order Without Explicit First Derivatives," Journal of Research, National Bureau of Standards, Vol. 54, pp. 119-125, 1955.

9. J. W. Leech, P. T. Hsu and E. W. Mack, "Stability of a Finite Difference Method for Solving Matrix Equations," AIAA J., Vol. 3, pp. 2172-2173, Nov., 1965.

10. C. M. Harris and C. E. Crede (ed.), Shock and Vibration Handbook, Vol. 1, pp. 8-53. McGraw-Hill, New York 1961.

11. J. S. Przemieniecki, Theory of Matrix Structural Analysis. McGraw-Hill, New York 1968.

12. S. P. Timoshenko, "Zur Frage Nach der Wirkung Eines Stosses auf Einen Balken," Zeits. Math. Phys., Vol. 62, pp. 198-209, 1913.

13. E. H. Lee, "The Impact of a Mass Striking a Beam," J. Applied Mechanics, Vol. 62, pp. A129-A138, 1940.

14. M. A. Dengler and M. Goland," Transverse Impact on Long Beams, Including Rotatory Inertia and Shear Effects," Proc. 1st. U.S. National Congress of Applied Mechanics, pp. 179-186, 1951.

15. D. M. Cunningham and W. Goldsmith, "An Experimental Investigation of Beam Stresses Produced by Oblique Impact of a Steel Sphere," J. Appl. Mech., Vol. 23, pp. 606-611, 1956.

16. W. Goldsmith and D. M. Cunningham, "Kinematic Phenomena Observed During the Oblique Impact of a Sphere on a Beam," J. Appl. Mech., Vol. 23, pp. 612-616, 1956.

17. W. Goldsmith, Impact. pp. 82-87. Edward Arnold Ltd., London, 1960.

18. R. M. Davies, "The Determination of Static and Dynamic Yield Stresses Using a Hard Steel Ball," Proc. of the Royal Soc. of London, Series A, Vol. 197, pp. 416-432, 1949.

19. K. E. Barnhart and W. Goldsmith, "Stresses in Beams During Transverse Impact," J. Appl. Mech., Vol. 24, pp. 440-446, 1957.

20. J. R. Willis, "Hertzian Contact of Anisotropic Bodies," J. Mech. Phys. Solids, Vol. 14, pp. 163-176, 1966.